Desalination and Water Treatment
www.deswater.com

doi:10.5004/dwt.2018.21999

103 (2018) 113–121
January

Removal of methylene blue from water by food industry by-products and biochars

Alexios G. Orfanos[a], Ioannis D. Manariotis[a,*], Hrissi K. Karapanagioti[b]

[a]*Environmental Engineering Laboratory, Department of Civil Engineering, University of Patras, 265 04 Patras, Greece, email: algeorfns@gmail.com (A.G. Orfanos), idman@upatras.gr, (I.D. Manariotis)*
[b]*Department of Chemistry, University of Patras, 265 04 Patras, Greece, email: karapanagioti@upatras.gr (H.K. Karapanagioti)*

Received 30 November 2017; Accepted 31 January 2018

ABSTRACT

The aim of this work was to evaluate the effectiveness of easily available food industry by-products for the removal of methylene blue (MB) from aqueous solutions. More specifically, malt spent root lets (MSR), coffee residues (KES) and their biochars were employed. The sorption of MB by pyrolyzed MSR was examined using materials pyrolyzed at temperatures ranging from 300 to 900°C. High surface areas for pyrolyzed MSR were observed at pyrolysis temperatures higher than 500°C, and the maximum surface area (300 m^2 g^{-1}) was observed for biochar MSR pyrolyzed at 850°C (MSR 850). Kinetic and isotherm experiments were conducted for the MSR, MSR 850 KES and KES pyrolyzed at 850°C (KES 850). According to kinetic experimental data, sorption capacities at 120 min were over 58% of their equilibrium values for all materials used. The maximum MB sorption capacities for MSR, MSR 850, KES, and KES 850 were 73, 130, 110, and 130 mg g^{-1}, respectively. Continuous flow-through column experiments were conducted with KES, and the maximum MB capacity was 114 mg g^{-1}.

Keywords: Biochar; Biosorbents; Sorption; Dyes; Methylene blue

1. Introduction

Dyes are categorized into reactive, disperse, direct, vat, sulfur, basic, acid and solvent dyes based on their usage or the method of application, and into azo, anthraquinone etc., based on their chemical structure [1]. More than 100,000 commercially available dyes, and over 7×10^5 tons of synthetic dyes are produced annually world-wide [2]. Since the occurrence of organic compounds in nature is analogous to their production [3], this increase in dye classes and quantities is alarming for the fate of dyes in the environment.

Depending on the class of the dye, the losses in wastewater can vary from 0 to 10% for basic dyes to as high as 50% for reactive dyes [4]. Even at low concentrations, dyes are visible in effluent, and the high light absorption affects the photosynthesis of aquatic species [5]. Most dyes are organic compounds, that increase the oxygen demand of the water bodies, and many of them are toxic and hazardous to aquatic organisms whereas their degradation products may be mutagenic and carcinogenic [6]. Methylene blue (MB) is a basic dye with various applications and is mostly used by industries involved in textile, paper, rubber, plastics, leather, cosmetics, pharmaceutical, and food sectors [7–9]. Basic dyes, like MB, are also considered as cationic dyes because they form a colored cationic salt when dissolved in water.

There are numerous treatment processes for effluent containing dyes like biodegradation, chemical oxidation, foam flotation, electrolysis, photocatalysis, electro-coagulation, adsorption and ultrasound [4,10]. Sorption is considered as one of the most effective processes due to its low cost, ease of operation and design simplicity [11,12]. Commercial activated carbon is a remarkable sorbent but it is expensive due to its high production cost [13]. Biochar is an alternative to activated carbon, and is a solid material produced by the carbonization of biomass under partial absence of oxygen [14]. The source materials usually are not activated or further treated before use [14], and biochar is less expensive than activated carbon [5,15]. Biochars produced from differ-

*Corresponding author.

ent organic wastes have been successfully tested to remove pollutants such as metals [14,16] and dyes [5]. The raw agricultural wastes can also be used as biosorbents, which may be more desirable due to lower production cost compared to activated carbon and biochars [17–19].

Malt spent rootlets (MSR) are biomaterials produced in big quantities by beer industry as by-products [20]. The average annual global production of brewers' spent grain is estimated to be about 39×10^6 tonnes [21]. Coffee is one of the most consumed beverages all over the world. In 2016 the production of coffee reached about 9×10^6 tonnes [22]. The processing of coffee often generates significant amounts of solid residues, which account for approximately 50% of the total input mass of coffee feedstock [23].

The aim of the present work was to evaluate the potential use of biochars produced from malt spent rootlets (MSR) and coffee residues (KES) to remove MB from pure aqueous solutions. The sorption capacity of the biochars compared with the raw materials used. Batch experiments were conducted to obtain the optimum sorption conditions under different MB concentrations and contact times. The effect of MSR pyrolysis temperature on MB sorption capacity was examined. Finally, the raw material with the highest sorption capacity (KES) was selected for further evaluation in continuous flow-through experiments.

2. Materials and methods

2.1. Sorbent materials

MSR were obtained from the Athenian Brewery S.A. (Patras, Greece). They were dried overnight at 50°C, and sieved. The size fraction of 0.150 to 1.180 mm was found to represent about 70% of the mass sieved, and was selected for the experiments of this study. KES was obtained after espresso coffee was brewed through coffee machines at the University of Patras coffee shops. MSR and KES were separately weighted and placed into ceramic vessels that were closed with their respective caps. These vessels were custom-made not to allow oxygen to enter the vessels at high temperatures. The vessels with the MSR were placed in a gradient temperature furnace (LH 60/12, Nabertherm GmbH, Germany) at temperatures ranging from 300 to 900°C (i.e. 300, 400, 500, 750, 850, 900°C). KES was pyrolyzed at 850°C. The mass of the MSR and KES was weighted before and after the pyrolysis process and the weight loss due to pyrolysis was calculated. The biochar MSR was powdered before sorption experiments. The surface area, the pore volume, and the average pore size of the biochars were determined using gas (N_2) adsorption–desorption with the Micromeritics TriStar 3000 Analyzer system using the Brunauer, Emmett, and Teller (BET) equation.

2.2. Methylene blue

High purity MB ($C_{16}H_{18}ClN_3S\ xH_2O$) was supplied by Alfa Aesar GmbH & Co. KG, Germany. A stock solution of 1000 mg L^{-1} was prepared by dissolving accurately weighed the dye in distilled water. The experimental solutions were prepared by diluting stock solution of MB with distilled water to the desired concentration. The pH of MB solution from an initial value of 5.5 was adjusted to 7.5 by drop wise addition of a 0.1 M NaOH solution and was measured with a pH meter (pH 310 meter, Oakton Instruments, Singapore). Previous studies have shown that the sorption capacity for MB was not affected at pH above 5 [5] or 7.5 [6]. MB concentration was determined by measuring the absorbance at 660 nm with a UV-VIS spectrophotometer (U1100, Hitachi). The calibration curve of MB solution covered a range from 0.5 to 10 mg L^{-1}.

2.3. Batch experiments

A small portion (10 mL) of the standard MB solution was transferred into 15 mL polypropylene test tubes containing 5 or 10 mg of sorbent. The tubes were placed on a rotator (J.P. Selecta, Spain) for a specified time in a dark room. Subsequently, the tubes were placed vertically for the sorbent to settle. MSR samples pyrolyzed at 300, 400, 500, 750, 850, and 900°C were tested at initial MB concentration of 50 mg L^{-1}, a sorbent dose of 0.5 g L^{-1} and contact time of 24 h.

Kinetic and isotherm experiments were conducted for the MSR, MSR pyrolyzed at 850°C (MSR850), KES, and KES pyrolyzed at 850°C (KES 850). For the kinetic experiments, the initial MB concentration was 50 mg L^{-1} for the MSR, MSR 850 and KES and 100 mg L^{-1} for the KES 850. The sorbent dose was 0.5 g L^{-1} for the KES, KES 850 and MSR 850 and 1 g L^{-1} for the MSR. Although it is much easier to make comparisons and appreciate the sorbents effectiveness when all experimental conditions are the same, the sorbent dose for MSR, and dye concentration for KES 850 were higher due to technical difficulties (i.e. grain size, detection limit). However, all results are reported and compared per unit mass of sorbent. The effect of contact time on MB sorption was examined at the range of 20 to 1440 min for the MSR based materials and at the range of 10 to 1440 min for the KES based materials. For the isotherm experiments, the initial MB concentrations were 50, 70, 100, 150 and 200 mg L^{-1} for the biochars and 20, 50, 100, 150, 200 mg L^{-1} for the raw materials. Based on the kinetic experiments results the contact time for each sorbent was set. More specifically, the contact time of KES based sorbents was 24 h, while for the MSR based sorbents was 5 h since a plateau was observed to occur earlier. All experiments were performed in duplicates at pH 7.5. Blanks without the presence of the sorbent were employed for all tests performed in order to account for any losses on the tube walls or due to the experimental conditions.

2.4. Column experiments

The raw material with the highest sorption capacity (KES) was selected for further evaluation in continuous flow-through experiments. A plexiglass column was filled with KES and was operated in an upflow-mode. The length of the sorbent packed zone was 12 cm, the internal diameter of the column 3 mm, the initial MB concentration 50 mg L^{-1} and the flow rate 0.5 mL min^{-1}. The concentration of the MB was measured in samples taken from the effluent. The points where the dye concentration in the effluent reached 5 and 90% were referred to as the breakthrough and exhaustion points, respectively.

3. Results and discussion

3.1. Effect of MSR pyrolysis temperature on sorption capacity

The experimental data presented in Fig. 1 clearly show that under the experimental conditions studied (C_0 = 50 mg L^{-1}, pH 7.5, and 24 h agitation), the removal of MB increases with increasing MSR pyrolysis temperature. The sorption capacity of MB (q) was low (9 to 12 mg MB g^{-1} biochar) for MSR pyrolyzed at temperatures ranging from 300 to 500°C, and considerably increased for MSR pyrolyzed at higher temperatures. The maximum removal of MB was 99 mg g^{-1} and was observed for MSR 850. Further increase of the pyrolysis temperature to 900°C resulted in lower sorption capacity than that for MSR850. The pyrolysis temperature significantly affected the surface area of the biochar. BET surface values ranged from 0.5 to 5.5 m^2 g^{-1} for temperatures from 300 to 500°C, respectively. At pyrolysis temperatures higher than 500°C, high surface areas were observed with a maximum surface area value (300 m^2 g^{-1}) at 850°C. As temperature increases pore blocking substances are thermally cracked, resulting in the formation of more small size pores [16]. The MB uptake was considerably affected by the biochar surface area, which increased with the pyrolysis temperature.

Regression analysis was applied to investigate the correlation between the q and BET surface. The dependence of q (mg g^{-1}) vs. BET area (m^2 g^{-1}) is expressed by the equation below and the R^2 = 0.955:

$$q = 10.6 + 0.319\,BET \quad (1)$$

In order to eliminate the observed heteroscedasticity of the response (higher values of the independent variable BET seems to cause a greater variability of q, which violates the assumption of homoscedasticity of the linear regression model), the weighted least squares (WLS) estimation method was used, in which the ordinary least squares is applied to transformed values of q and BET. The observed heteroscedasticity suggests the transformation $q^* = q/BET$ for the dependent and 1/BET for the independent variable [24]. The dependence of plot of $q^*(q/BET)$ vs. (1/BET) is expressed as:

$$\frac{q}{BET} = 0.246 + 10.4\frac{1}{BET} \quad (2)$$

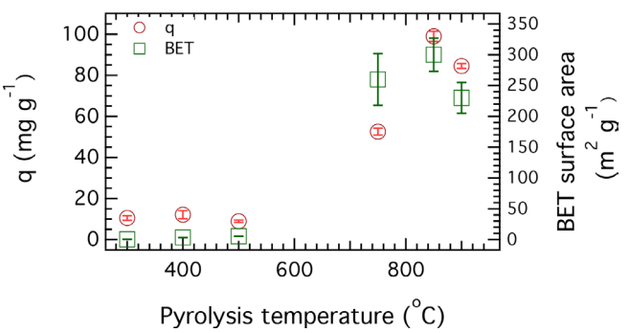

Fig. 1. Effect of pyrolysis temperature of MSR on MB removal after 24 h mixing at C_0 = 50 mg L^{-1} and pH 7.5. Error bars represent standard deviation of duplicates.

The R^2_{WLS} value of the transformed variables is 0.999 and the p-value associated with the F-test is <0.001, implying that *1/BET** reliably predicts *q/BET*. The R^2_{WLS} cannot be compared directly with the initial R^2 since R^2_{WLS} is the proportion of the variance in the transformed dependent variable that is explained from the transform independent variable. It will be wiser to compute the R^2 based on the residuals of the regression line [25], suggested by the aforementioned model for the expected value of q given by:

$$q = 10.4 + 0.246\,BET \quad (3)$$

The pseudo-R^2 for this model is 0.86. This pseudo-R^2 may be smaller than the original R^2 but at least the assumption of homoscedasticity of the linear regression model is not violated.

3.2. Effect of contact time

The effect of contact time on MB removal for the four materials used is shown in Fig. 2. As can be seen from the plots, fast kinetics were observed within the initial 60 min reflecting immediate MB uptake or sorption on the external surface of the sorbent particles. A plateau was observed for MSR after 120 min and the sorption capacity was about 40 mg g^{-1}. MSR850 exhibited significantly greater sorption capacity that after 120 min it reached a plateau at 94 mg g^{-1}. The higher capacity is attributed to the higher surface area of MSR850 than MSR. KES was more effective to remove MB than MSR, and after 120 min a sorption capacity of 64 mg g^{-1} was achieved. Although during the first 60 min KES and KES 850 exhibited similar sorption efficiencies, the sorption capacity of KES 850 increased with time and after 24 h it reached 120 mg g^{-1} of MB compared to 85 mg g^{-1} of MB for KES. For KES 850 a first plateau was observed between 120 and 360 min and a second plateau was observed after 960 min contact time.

3.3. Sorption kinetics

The estimation of kinetic parameters will provide important information for the sorption process in case an

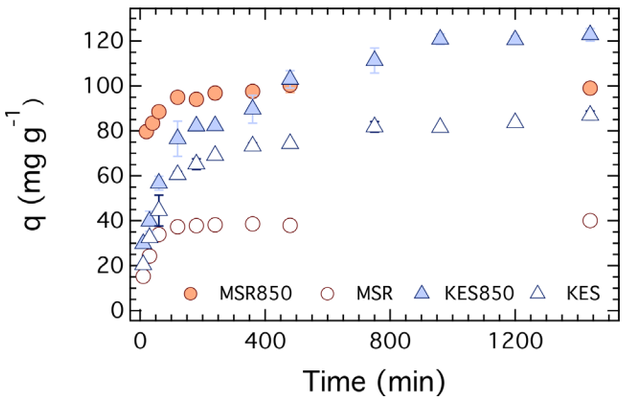

Fig. 2. Effect of contact time on MB sorption. Initial MB concentration was 50 mg L^{-1} for KES, MSR and MSR850 and 100 mg L^{-1} for KES 850, and pH 7.5.

engineering system will be designed (e.g. filter design, flow rate, etc). The pseudo-first-order model and the pseudo-second-order model were applied to investigate the kinetics of MB sorption for the four materials studied. The pseudo-first-order equation as suggested from Lagergen [26] is:

$$\frac{dq}{dt} = k_1\left(q_e - q_t\right) \tag{4}$$

where q_e (mg g^{-1}) and q_t (mg g^{-1}) are the quantity of MB sorbed per mass unit of biochar at equilibrium and at a given time t, respectively, and k_1 (min^{-1}) is the first-rate constant. Integration and rearrangement of Eq. (4) gives the following linear form:

$$\ln\left[q_e - q_t\right] = \ln\left[q_e\right] - k_1 t \tag{5}$$

The values of k_1 and q_e can be determined by the slope of the linear plot of $ln(q_e - q_t)$ vs. t (Fig. 3).

The expression of the pseudo-second-order rate based on the solid capacity has been presented by Blanchard et al. [27] as follows:

$$\frac{dq}{dt} - k_2\left(q_e - q_t\right)^2 \tag{6}$$

where k_2 is the rate constant (g mg^{-1} L^{-1}). The integration of Eq. (4) gives:

$$\frac{t}{q_t} = \frac{1}{k_2 {q_e}^2} + \frac{1}{q_e} t \tag{7}$$

where k_2 is the second-order rate constant (g/mg·min). The linear plots of $\frac{t}{q_t}$ vs. t give $\frac{1}{q_e}$ as the slope and $\frac{1}{k_2 qe^2}$ as the intercept (Fig. 3).

The kinetic parameters related to the pseudo first-order and the pseudo second-order kinetic models employed in this study, together with the fitted parameters are given in Table 1. The suitability of the kinetic models can be assessed by both the correlation coefficient (R^2) and the residual sum of squares (RSS):

$$RSS = \sum_{i=1}^{n}\left(q^{exp} - q^{calc}\right)^2 \tag{8}$$

where q^{exp} and q^{calc} are the experimental and predicted by the model values of q (mg g^{-1}), respectively, n is the number of experimental values, and the subscript $i = 1…n$ indicates the corresponding sample.

The pseudo first-order kinetic model does not fit well the experimental data (Fig. 3a), and the model does not give reasonable values for q_e. The experimental data of the MSR 850 fitted better than the corresponding raw material and fitted similarly for KES and KES 850. This finding may suggest that the sorption process for MSR does not follow the pseudo-first-order sorption rate expression of Lagergren. The experimental data were fitted well by the pseudo second-order kinetic model and the plot of t/q vs. t gave a straight line (Fig. 3b). The R^2 values of the pseudo second-order model exceeded 0.995 for all the materials tested. Moreover, the pseudo second-order model presented quite lower RSS values than the pseudo first-order model, for the four sorbents. The calculated values of q_e based on the second-order model were close to the experimental values, and were significantly different from the q_e values based on the first-order model. Regarding the sorbents, the q_e values are greater for the biochars than for their corresponding raw materials. In both kinetic models, the k values were greater

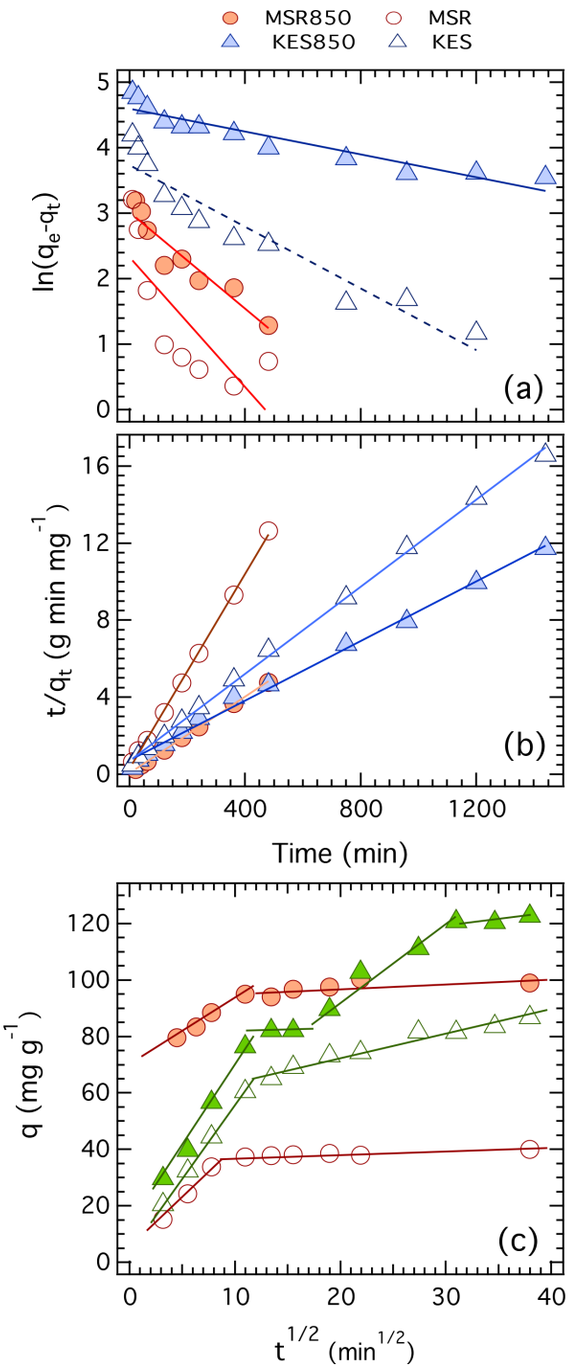

Fig. 3. Kinetic models of MB sorption: (a) Pseudo first-order, (b) Pseudo second-order, (c) Intraparticle diffusion. Initial MB concentration 50 mg L^{-1} for KES, MSR and MSR850 and 100 mg L^{-1} for KES850, and pH 7.5.

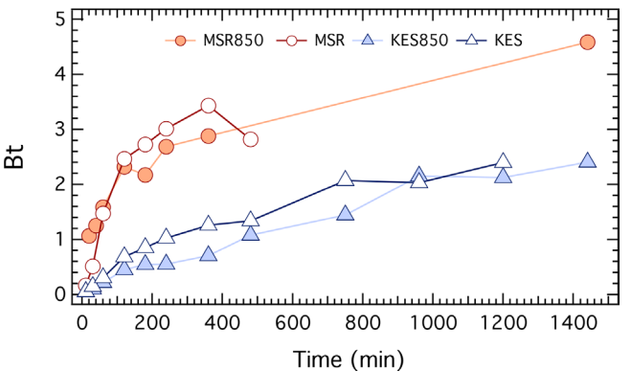

Fig. 4. Bt vs. time for the four materials examined.

Table 1
Pseudo first and pseudo second-order kinetic models' constants

Kinetic model	Material			
	MSR850	MSR	KES850	KES
Pseudo first-order				
k_1 (min^{-1})	0.0037	0.005	0.0009	0.0024
q_e (mg g^{-1})	20.4	10.28	99.44	42.06
R^2	0.899	0.601	0.886	0.915
RSS	105	289	1136	22961
Pseudo second-order				
k_2 (g mg^{-1} min^{-1})	1.1×10^{-3}	2.2×10^{-3}	8.15×10^{-5}	1.83×10^{-4}
q_e (mg g^{-1})	101.01	39.37	129.9	88.50
R^2	0.999	0.999	0.995	0.998
RSS	74	29	114	788

for the MSR than for the KES based materials. Finally, comparing the two models, lower k values were shown at the second-order model. This suggested that the overall rate of MB sorption process appeared to be controlled by chemical processes [28]. The pseudo-second-order kinetic model has been reported to better fit the experimental data is reported for the sorption of MB by various sorbents like *Paspalum notatum* [29], ground palm kernel coat [30], surface modified *Strychnos potatorum* seeds [13], poly(amic acid)-modified chitosan [31] and biochars prepared from anaerobic digestion residue, palm bark, and eucalyptus [5].

3.4. Diffusion based kinetic models

The sorption of a solute present in a solid-solution system is usually assumed to consist of the following steps [26,32,33]: (i) bulk diffusion, (ii) external mass transfer of sorbate molecules across the boundary liquid film around the sorbent particles, (iii) binding of sorbate molecules on the active sites on the surface of the sorbent particles, (iv) intra-particle diffusion of sorbate molecules into sorbent pores (macro, meso and nano), and (v) sorption and desorption of sorbate molecules on the active sites distributed on the external surface of and within the sorbent particles. Generally, the steps involving binding (iii) and sorption (v) are rapid and can be neglected when evaluating the rate-determining step of the sorption process. The overall rate of sorption will be controlled by the slowest step, which would be either external mass transfer or intraparticle diffusion [34].

In order to identify the diffusion mechanism the Weber-Morris intraparticle diffusion model [35] was applied for the four materials:

$$q_t = k_{id} t^{\frac{1}{2}} + C \tag{9}$$

where k_{id} is the intraparticle diffusion rate constant (mg g^{-1} min$^{-1/2}$), which is estimated from the slope of the linear plot of q_t vs. $t^{1/2}$, and C is (mg g^{-1}) the y-intercept. High C values are indicative of external mass transfer thereby acting as a rate-controlling step [36]. If the plot of q_t vs. $t^{1/2}$ gives a straight line intra particle diffusion is involved in the sorption rate and if the straight line cross the origin intraparticle diffusion is the rate limiting step [36,37]. The Weber-Morris plots of the experimental data are shown in Fig. 3c. The plot of MSR and MSR850 consists of two parts, while the KES and KES 850 plots consist of two and four parts, respectively. The break points, the sorption capacity at the end of the break point, the k_{id}, the y-intercept (C), the correlation coefficient and the residual sum of squares of the preceded to break point line are tabulated in Table 2. The high R^2 and low RSS values show that the chosen lines fitted well the experimental data in the different parts of the plots. The intercept in the first linear part, C, was not equal to zero for all four materials tested implying that intra-particle diffusion was not the rate-controlling step, and that mass transfer took place by boundary layer diffusion. More specifically the average values of the intercept of the first linear part of the MSR, MSR 850, KES and KES 850 were 2.13 ± 0.62, 69.6 ± 0.38, 4.24 ± 2.01 and 8.78 ± 2.03, respectively. During the first linear part the sorption efficiency for MSR and MSR850 was quite high and reached values of 85 and 95%, respectively. However, MSR and MSR 850 in the second linear part exhibited k_{id} values close to zero, which implies that intraparticle diffusion was the rate limiting step after 60 and 120 min for the MSR and MSR 850, respectively. A different trend was observed with the coffee-based materials. The first linear part for both KES and KES 850 covered a time period up to 144 min and the sorption of MB was 75 and 65% for the KES and KES 850, respectively. The second linear part for KES accounted for a very small increase of MB removal. It is interesting to note that the first break point of the coffee materials occurred at the same time (144 min), while the first break point for the MSR based materials was different (60 and 120 min for MSR and MSR850, respectively.

According to the literature the multi linearity is often observed when different mechanisms are involved in sorption process. The linear segments may be attributed to the variation of internal pore sizes [38]. Cheung et al., 2008 [39] observed multi linearity during the sorption of acid dye onto chitosan. More specifically, they observed three steps; the first segment was attributed to the diffusion of dye through the solution to the external surface of sorbent, in the second segment the intraparticle diffusion was the rate limiting step, and in the third intraparticle diffusion

Table 2
Intra particle diffusion constants

Material	Break point (min)	q (mg g^{-1})	k_{id} (mg g^{-1} min$^{-1/2}$)	C (mg g^{-1})	R^2	RSS
MSR850	120	95	2.41	68.9	0.989	1.48
MSR	60	34	4.06	2.32	1	0.08
KES850	144	80	6.13	8.8	0.992	9.66
	289	82	0.07		1	0
	960	121	2.40		0.959	21.2
KES	144	65	5.15	4.24	1	0.18

started to decrease due to the low concentration left in the solution.

To estimate the actual rate-limiting step involved in the sorption process, the experimental data were further analyzed by the Boyd model [40]. This model assumes that the main resistance to diffusion is the boundary layer surrounding the particle and is expressed as:

$$F(t) = 1 - \left(\frac{6}{\pi^2}\right)\sum_{m=1}^{\infty}\left(\frac{1}{m^2}\right)e^{-m^2Bt} \quad (10)$$

where $F(t)$ is the fraction of the solute sorbed at different times t:

$$F(t) = \frac{q}{q_e} \quad (11)$$

where q and q_e are the dye uptake (mg g^{-1}) at time t and at equilibrium, respectively, m is the number of particles, and B is obtained from the following equation:

$$B = \frac{D_i\pi^2}{r^2} \quad (12)$$

where D_i is the internal diffusion coefficient and r is the radius of sorbent particle.

Reichenberg, 1953 [41] after applying Fourier transform and integration, managed to obtain the following approximations:

$$\text{for F(t)} > 0.85,\ Bt = -0.4977 - In\left(1 - F(t)\right) \quad (13)$$

while for F(T) < 0.85,

$$Bt = 2\pi - \frac{\pi^2 F(t)}{3} - 2\pi\sqrt{1 - \frac{\pi F(t)}{3}} \quad (14)$$

If the plot of Bt against time is linear and passes through the origin the intraparticle diffusion controls the rate of mass transfer, while if the plot is nonlinear or linear but does not pass through the origin the film diffusion or chemical reaction control the sorption rate [40,41]. In the present work the Boyd plot consisted of more than one linear segment (Fig. 4). The plots of MSR, MSR 850, KES and KES 850 are nonlinear. The coffee based materials show greater linearity than the MSR based materials. The intercepts of KES (0.002), KES 850 (0.01) and MSR (0.01) are closer to zero compared

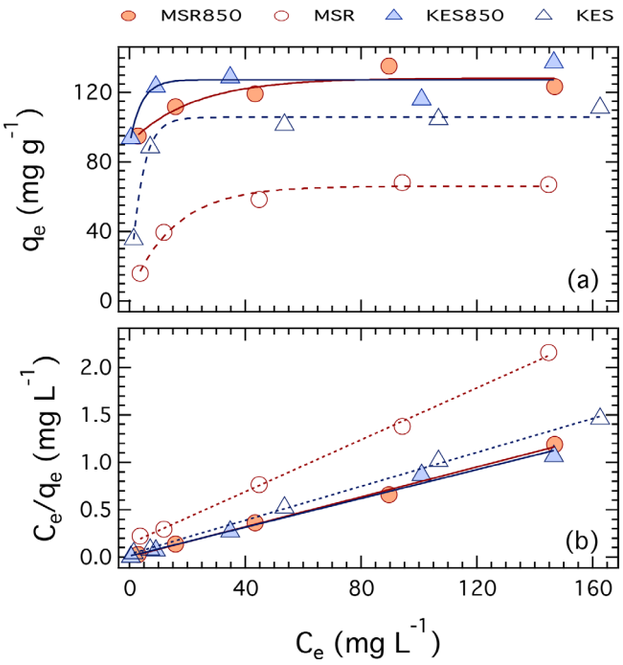

Fig. 5. MB uptake by the four materials tested at initial concentrations from 20 to 200 mg L^{-1}, solid to liquid ratio of 1 g L^{-1} for MSR and 0.5 g L^{-1} for the other sorbents, and contact time of 5 h for the MSR based sorbents and of 24 h for the KES based sorbents: (a) experimental data, (b) linearized form of the Langmuir model equation.

to MSR 850 (0.8), which implies that intraparticle diffusion is more important. In similar studies, film diffusion was the rate-limiting step at the biosorption of MB using *Paspalum notatum* [29] and rice husk [32].

3.5. Sorption Isotherms

The maximum sorption capacity was estimated by fitting the experimental data with the non-linear models, Freundlich and Langmuir. The two models linear forms are:

$$\frac{C_e}{q_e} = \frac{1}{q_{\max}k_L} + \frac{C_e}{q_{\max}} \quad (15)$$

$$Inq_e = Ink_F + N\,InC_e \quad (16)$$

where C_e (mg L^{-1}) is the equilibrium concentration in the solution, q_{max} (mg g^{-1}) is the maximum sorption capacity, K_L is the constant of Langmuir model (L mg^{-1}) related to binding energy for sorption, k_F ((mg g^{-1})(L mg^{-1})^N) is the sorption constant for Freundlich model, and N is the Freundlich exponent related to sorption nonlinearity, indicative of the distribution of the active sites on the sorbent. The experimental results and the linearized Langmuir isotherm model are illustrated in Fig. 5.

The fitting of the experimental results (R^2 from 0.732 to 0.897) indicated that the application of the Freundlich isotherm model did not adequately fit the experimental data (Table 3). The Langmuir isotherm model matched

better the experimental results (R^2 from 0.987 to 0.999), for all materials used indicating a limited number of sorption sites. A comparison of the maximum sorption capacity of biosorbents and the derived biochars or activated carbons is presented in Table 4. Some of the q_{max} values for biosorbents such as of peat and activated carbons are significantly higher than those of biochar and of the biosorbents studied in the present study. However, q_{max} values of KES, KES 850, and MSR 850 are comparable with those of most similar materials. The Langmuir isotherm model was also the appropriate model for the description of MB sorption by various sorbents like tea wood bark [43], walnut and cherry sawdust [46], and jute fiber carbon [49].

Table 3
Isotherm model parameters for methylene blue sorption

Isotherm model	Material			
	MSR850	MSR	KES850	KES
Langmuir model				
q_{max} (mg g^{-1})	127	73	132	112
K_L (L mg^{-1})	1.1	0.09	0.54	0.27
R^2	0.996	0.998	0.987	0.999
Freundlich model				
K_F [(mg g^{-1})(L $mg^{-1})^N$]	89	12	102	42
N	0.08	0.38	0.05	0.21
R^2	0.868	0.897	0.732	0.792

3.6. Column studies

The breakthrough data of the column experiments are presented in Fig. 6 as the dimensionless concentration ratio (C/C_0) with time. The column had been packed with 0.36 g KES, and the t_{bk} for MB was 19.6 h, which corresponds to about 692 bed pore volumes. The time required for the effluent to reach 90% of the influent concentration was 36.4 h. The equilibrium uptake of MB in the column (q_{eq}) can be estimated from the following equation [47]:

$$q_{eq=}\frac{\left(QC_{influent}10^{-3}\right)\int_0^t\left(1-\left(C_t-C_{influent}\right)\right)dt}{M} \quad (17)$$

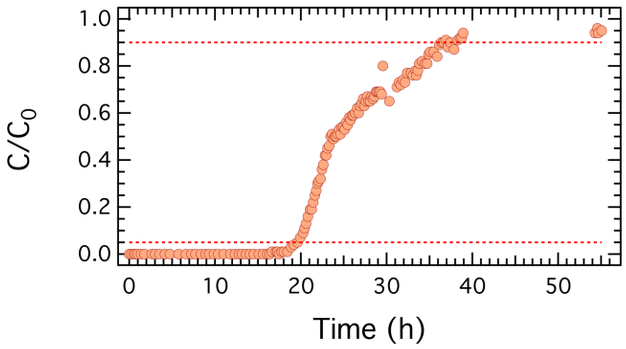

Fig. 6. Breakthrough curves of MB removal by KES. MB initial concentration 50 mg L^{-1}, flow rate 0.5 mL min^{-1} and pH 7.0.

Table 4
Maximum sorption capacity of various biosorbents and their corresponding biochars or activated carbon for MB

Sorbent	q_{max} (mg g^{-1})	Reference
Orange peel	18.6	Annadurai et al., 2002 [42]
Srychnos potatorum seeds surface modified	78.8	Senthamarai et al., 2013 [13]
Chitosan modified	392	Xing and Li, 2014 [18]
Tea wood bark	915	Mckay et al., 1999 [43]
Raw eucalyptus bark	204.08	Afroze et al., 2015 [44]
Watermelon rind	243.9	Lakshmipathy and Sarada, 2015 [45]
Walnut sawdust	59.2	Ferero, 2007 [46]
Cherry sawdust	39.8	Ferero, 2007 [46]
Cedar sawdust	142	Dotto et al., 2015 [47]
Peat	324	Fernandes et al., 2007 [48]
Jute fiber activated carbon	226	Senthilkumaar et al., 2005 [49]
Hazelnut husk activated carbon	476.2	Karaçetin et al., 2014 [11]
Spent activated clay	128	Weng and Pan, 2007 [50]
Spent coffee grounds	18.7	Franca et al., 2009 [51]
Raw coffee	112	This study
Biochar from coffee	132	This study
Malt spent rootlets (untreated)	73	This study
Biochar from malt spent rootlets	127	This study

where q_{eq} is in (mg g^{-1}), Q is the flow rate (mL min^{-1}), $C_{influent}$ and C_t (mg L^{-1}) is the concentration at the influent and at time t, and M is the mass of KES (g) in the column. The integral of Eq. (17) was estimated from time zero to the time that 90% of the influent MB concentration was found in the effluent. The maximum capacity of the column, q_{max} was 114 mg g^{-1}, which was close to the Langmuir sorption capacity (q_{max} = 112 mg g^{-1}). Dotto et al., 2015 [47] conducted fixed bed studies using ultrasonic surface modified chitin supported on sand for MB removal and reported column q_{max} of 51.8 mg g^{-1}.

4. Conclusions

The pyrolysis temperature of MSR significantly affected the high specific surface area and the optimum temperature was at 850°C for both the surface area and the sorption capacity. At 850°C the sorption capacity of MSR 850 was 74% higher than that of MSR. The pyrolysis of KES at 850°C resulted in higher maximum sorption capacity by 18%. Column experiments conducted with KES showed that MB concentration was below 5% of the influent concentration after 692 bed volumes, and non-equilibrium conditions do not seem to affect the sorption capacity of the sorbent. MSR and KES and their corresponding biochars seem to be suitable candidates for the removal of MB from aqueous solutions.

Acknowledgements

The authors would like to thank Polychronis Economou from the Civil Engineering Department of University of Patras for his helpful comments on statistical analysis.

References

[1] K. Hunger, Industrial Dyes: Chemistry, Properties, Applications, 1st edition. Wiley-VCH, Weinheim, Cambridge, 2003.
[2] M. Rafatullah, O. Sulaiman, R. Hashim, A. Ahmad, Adsorption of methylene blue on low-cost adsorbents: A review, J. Hazard. Mater., 177 (2010) 70–80.
[3] R.I. Schwarzenbach, P.M. Gschwend, D.M. Imboden, Environmental Organic Chemistry Wiley, New York, NY, 1993.
[4] O.J. Hao, H. Kim, P-C. Chiang, Decolorization of wastewater, Crit. Rev. Env. Sci. Technol., 30 (2000) 449–505.
[5] L. Sun, S. Wan, W. Luo, Biochars prepared from anaerobic digestion residue, palm bark, and eucalyptus for adsorption of cationic methylene blue dye: Characterization, equilibrium, and kinetic studies, Bioresource Technol., 140 (2013) 406–413.
[6] S. Banerjee, M.C. Chattopadhyaya, V. Srivastava, Y.C. Sharma, Adsorption studies of methylene blue onto activated saw dust: kinetics, equilibrium, and thermodynamic studies, Environ. Prog. Sust. Energy, 33 (2013) 790–799.
[7] E.S. Dragan, D.F.A. Loghin, Enhanced sorption of methylene blue from aqueous solutions by semi-IPN composite cryogels with anionically modified potato starch entrapped in PAAm matrix, Chem. Eng. J., 234 (2013) 211–222.
[8] L.S. Oliveira, A.S. Franca, T.M. Alves S.D.F. Rocha, Evaluation of untreated coffee husks as potential biosorbents for treatment of dye contaminated waters, J. Hazard. Mater., 155 (2008) 507–512.
[9] V.K. Gupta, R. Kumar, A. Nayak, T.A. Saleh, M.A. Barakat, Adsorptive removal of dyes from aqueous solution onto carbon nanotubes: A review, Adv. Colloid Interface Sci., 193–194 (2013) 24–34.
[10] M. Matouq, Z. Al-Anber, N. Susumu, T. Tagawa, H. Karapanagioti, The kinetic of dyes degradation resulted from food industry in wastewater using high frequency of ultrasound, Sep. Purif. Technol., 135 (2014) 42–47.
[11] G. Karaçetin, S. Sivrikaya, M. Imamoğlu, Adsorption of methylene blue from aqueous solutions by activated carbon prepared from hazelnut husk using zinc chloride, J. Anal. Appl. Pyrolysis., 110 (2014) 270–276.
[12] A. Bhatnagar, M. Sillanpää, Utilization of agro-industrial and municipal waste materials as potential adsorbents for water treatment - A review, Chem. Eng. J., 157 (2010) 277–296.
[13] C. Senthamarai, P.S. Kumar, M. Priyadharshini, P. Vijayalakshmi, V.V. Kumar, P. Baskaralingam, K.V. Thiruvengadaravi, S. Sivanesan, Adsorption behavior of methylene blue dye onto surface modified Strychnos potatorum Seeds, Environ. Prog. Sust. Energy, 32 (2013) 624–632.
[14] L.G. Boutsika, H.K. Karapanagioti, I.D. Manariotis, Aqueous mercury sorption by biochar from malt spent rootlets, Water Air Soil Pollut., 225 (2014) 1805.
[15] Y. Qiu, Z. Zheng, Z. Zhou, G.D. Sheng, Effectiveness and mechanisms of dye adsorption on a straw-based biochar, Biores. Technol., 100 (2009) 5348–5351.
[16] I.D. Manariotis, K.N. Fotopoulou, H.K. Karapanagioti, Detailed characterization of biochar sorbents produced from malt spent rootlets, Ind. Eng. Chem. Res., 54 (2015) 9577–9584.
[17] V.A. Anagnostopoulos, I.D. Manariotis, H.K. Karapanagioti, C.V. Chrysikopoulos, Removal of mercury from aqueous solutions by malt spent rootlets, Chem. Eng. J., 213 (2012) 135–141.
[18] Y. Xing, S. Li, Biosorption of methylene blue from aqueous solution by poly(amic acid)-modified chitosan, Environ. Prog. Sust. Energy, 33 (2014) 1180–1186.
[19] V. Anagnostopoulos, B. Symeopoulos, K. Bourikas, A. Bekatorou, Biosorption of U(VI) from aqueous systems by malt spent rootlets: kinetic, equilibrium and speciation studies, Int. J. Environ. Sci. Technol., 13(1) (2016), 285–296.
[20] S. Valili, G. Siavalas, H.K. Karapanagioti, I.D. Manariotis, K. Christanis, Phenanthrene removal from aqueous solutions using well-characterized, raw, chemically treated, and charred malt spent rootlets, J. Environ. Manage., 128 (2013) 252–258.
[21] K.M. Lynch, E.J. Steffen, E.K. Arendt, Brewers' spent grain: a review with an emphasis on food and health, J. Institute Brewing, 122 (2016) 553–568.
[22] ICO, 2016. http://www.ico.org/prices/po-production.pdf (Data as at 6 January 2017). Last visited May 27, 2017.
[23] S.M. Lamine, C. Ridha, H-M. Mahfoud, C. Mouad, B. Lotfi, A.H. Al-Dujaili, Chemical activation of an activated carbon prepared from coffee residue, Energy Procedia., 50 (2014) 393–400.
[24] N.R. Draper, H. Smith, Applied Regression Analysis (3rd edition). New York: Wiley 1998.
[25] J.B. Willett, J.D. Singer, Another cautionary note about R2: its use in weighted least-squares regression analysis, The American Statistician, 61 (1988) 236–238.
[26] Y.S. Ho, J.C.Y. Ng, G. McKay, Kinetics of pollutants sorption by biosorbents: A review, Sep. Purif. Methods, 29(2) (2000) 189–232.
[27] G. Blanchard, M. Maunaye, G. Martin, Removal of heavy metals from waters by means of natural zeolites, Water Res., 18 (1984) 1501–1507.
[28] Y.-S. Ho, Review of second-order models for adsorption systems, J. Hazard. Mater., B 136 (2006) 681–689.
[29] K.V. Kumar, K. Porkodi, Mass transfer, kinetics and equilibrium studies for the biosorption of methylene blue using Paspalum notatum, J. Hazard. Mater., 146 (2007) 214–226.
[30] N.A. Oladoja, C.O. Aboluwoye, Y.B. Oladimeji, Kinetics and isotherm studies on methylene blue adsorption onto ground palm kernel coat, Turkish J. Eng. Environ. Sci., 32 (2008) 303–312.
[31] M. Berrios, M.Á. Martín, A. Martín, Treatment of pollutants in wastewater: Adsorption of methylene blue onto olive-based activated carbon, J. Ind. Eng. Chem., 18 (2012) 780–784.

[32] N. Kannan, M.M. Sundaram, Kinetics and mechanism of removal of methylene blue by adsorption on various carbons—a comparative study, Dyes Pigments, 51 (2001) 25–40.
[33] D. Kumar, J.P. Gaur, Chemical reaction- and particle diffusion-based kinetic modeling of metal biosorption by a Phormidium sp.-dominated cyanobacterial mat. Biores. Technol., 102 (2011) 633–640.
[34] G. McKay, The adsorption of dyestuffs from aqueous solution using activated carbon: Analytical solution for batch adsorption based on external mass transfer and pore diffusion, The Chem. Eng. J., 27 (1983) 187–196.
[35] W.J. Weber, J.C. Morris, Kinetics of adsorption on carbon from solution, J. Sanit. Eng. Div., 89 (1963) 31–60.
[36] J. Chen, Y. Cai, M. Clark, Y. Yu, Equilibrium and kinetic studies of phosphate removal from solution onto a hydrothermally modified oyster shell material, PLoS One, 8 (2013) 1–10.
[37] K.G. Bhattacharyya, A. Sharma, Azadirachta indica leaf powder as an effective biosorbent for dyes: A case study with aqueous Congo Red solutions, J. Environ. Manage., 71 (2004) 217–229.
[38] Y.S. Ho, G. McKay, The kinetics of sorption of basic dyes from aqueous solution by sphagnum moss peat, The Canadian J. Chem. Eng., 76 (1998) 822–827.
[39] W.H. Cheung, Y.S. Szeto, G. McKay, Intraparticle diffusion processes during acid dye adsorption onto chitosan, Biores. Technol., 98 (2007) 2897–2904.
[40] G.E. Boyd, A.W. Adamson, L.S.Jr. Myers, The exchange adsorption of ions from aqueous solutions by organic zeolites. II. Kinetics, J. Am. Chem. Soc., 69 (1947) 2836–2848.
[41] D. Reichenberg, Properties of ion-exchange resins in relation to their structure. III. Kinetics of exchange, J. Am. Chem. Soc., 75 (1953) 589–597.
[42] G. Annadurai, R.S. Juang, D.J. Lee, Use of cellulose- based wastes for treatment of wastewater contaminated with dye and other organics, Biores. Technol., 92 (2002) 263–274.
[43] G. Mckay, J.F. Porter, G.R. Prasad, The removal of dye colours from aqueous solutions by adsorption on low-cost materials, Water Air Soil Pollut., 114 (1999) 423–438.
[44] S. Afroze, T.K. Sen, M. Ang, H. Nishioka, Adsorption of methylene blue dye from aqueous solution by novel biomass Eucalyptus sheathiana bark: equilibrium, kinetics, thermodynamics and mechanism, Desalin. Water Treat., 57 (13) 2016.
[45] R. Lakshmipathy, N.C. Sarada, Methylene blue adsorption onto native watermelon rind: bath and fixed bed column studies, Desal. Water Treat., 57 (23) 2016.
[46] F. Ferrero, Dye removal by low cost adsorbents: Hazelnut shells in comparison with wood sawdust, J. Hazard. Mater., 142 (2007) 144–152.
[47] G.L. Dotto, J.M. Nascimento dos Santos, R. Rosa, L.A.A. Pinto, F.A. Pavan, E.C. Lima, Fixed bed adsorption of methylene blue by ultrasonic surface modified chitin supported on sand, Chem. Eng. Res. Design., 100 (2015) 302–310.
[48] A.N. Fernandes, C.A.P. Almeida, C.T.B. Menezes, N.A. Debacher, M.M.D. Sierra, Removal of methylene blue from aqueous solution by peat, J. Hazard. Mater., 144 (2007) 412–419.
[49] S. Senthilkumaar, P.R. Varadarajan, K. Porkodi, C.V. Subbhuraam, Adsorption of methylene blue onto jute fiber carbon: Kinetics and equilibrium studies, J. Colloid Interface Sci., 284 (2005) 78–82.
[50] C.H. Weng, Y.F. Pan, Adsorption of a cationic dye (methylene blue) onto spent activated clay, J. Hazard. Mater., 144 (2007) 355–362.
[51] A.S. Franca, L.S. Oliveira, M.E. Ferreira, Kinetics and equilibrium studies of methylene blue adsorption by spent coffee grounds, Desalination, 249 (2009) 267–272.